Description of superdeformed nuclei in the $A \sim 190$ region by generalized deformed $su_q(2)$

H. H. Alharbi[*]
National Center for Mathematics and Physics, KACST, P. O. Box 6086, Riyadh 11442, Saudi Arabia

H. A. Alhendi[†] and F. S. Alhakami
Department of Physics and Astronomy, College of Science, King Saud University, P. O. Box 2455, Riyadh 11454, Saudi Arabia
(Received 5 November 2008; published 20 May 2009)

The generalized deformed $su_q(2)$ model is applied to 79 superdeformed bands in the region $A \sim 190$. The transition energies and the moments of inertia are calculated within the model and their validity is investigated by comparing them with the experimental data. Both the standard $su_q(2)$ and the generalized one fail to account for the uprising and the downturn of the dynamic moments of inertia. Both models, however, show remarkable agreement with the available experimental data at low angular frequancy ($\hbar\omega \leqslant 0.25$ MeV).

DOI: 10.1103/PhysRevC.79.054324 PACS number(s): 21.10.Re, 21.60.Fw, 27.80.+w

I. INTRODUCTION

Superdeformed nuclei were first observed in fission isomers in the actinide region [1]. A theoretical explanation of the occurrence of fission isomers, based on shell effect corrections on the liquid drop potential energy surface, was, at that time, offered by Strutinsky [2]. The main result was the possible existence of a second minimum in the potential energy as a function of nuclear deformation. It is expected nowadays that a third minimum may occur corresponding to hyperdeformed nuclei [3].

A superdeformed rotational band in ^{152}Dy in the form of a series of γ-ray energies was first populated in the heavy-ion fusion-evaporation reaction ^{108}Pd(^{48}Ca,4n)^{152}Dy [4]. Since then extensive experimental and theoretical studies have been undertaken. At present superdeformed bands have been observed in various atomic mass regions [5]. The most notable regions are at $A \sim 130$, 150, and 190 in which axis ratios are, respectively, close to 1.5:1, 2:1, and 1.7:1 [6].

Superdeformed nuclei enjoy several characteristics that make them of particular interest theoretically and experimentally. In addition to their extreme shape and stability against fission, they show great regularity in their rotational bands and exhibit some type of universal phenomenon in relation to the existence of nearly identical bands in pairs of nuclei in different mass regions and as a result their dynamic moments of inertia are approximately similar [7]. It is expected that the process of the decay of superdeformed nuclei to normal deformed nuclei could proceed through quantum tunneling [8].

For high spin, superdeformed rotational spectra follow, in general, approximately that of a rigid rotor. Hence the kinematics and the dynamic moments of inertia are nearly constant with slight gradual increases with angular momentum, at low angular frequency. At high angular frequency, the dynamic moments of inertia show irregular behavior.

In this work we consider the q deformation of the enveloping Lie algebra $su_q(2)$ [9], which has recently attracted much interest for the calculation of rotational spectra of deformed [10] and superdeformed nuclei [11]. The validity of the standard $su_q(2)$ model has, however, been recently questioned [12]. A generalized form of the model that is obtained by replacing the angular momentum spectral expression $I(I+1)$ by $I(I+c)$ has been used to describe successfully the vibrational, transitional, and rotational nuclear spectra of well-deformed nuclei [13]. Here we apply this generalized form to the calculation of the rotational transition energies, the kinematic moments of inertia, and the dynamic moments of inertia for 79 superdeformed energy bands in the region $A \sim 190$ and compare the results with the experimental data. A sensitive measure of the applicability of a model to superdeformed bands is the dynamic moment of inertia. This is because it is inversely proportional to the difference of the transition energies and these transition energies are closely spaced. The model results show remarkable agreement with the experimental data in the rotational region at low angular frequency ($\hbar\omega \leqslant 0.25$ MeV). A comparison with the standard $su_q(2)$ model is also made. It is also shown that in addition to the previously predicted deviation of the standard $su_q(2)$ in the case of deformed nuclei, the standard and generalized deformed $su_q(2)$ do deviate for the case of the superdeformed nuclei considered in this work. It is also concluded, contrary to the expectation of Ref. [13], that in the rotational region the generalized $su_q(2)$ does not in general coincide with the standard one.

In the following section we present a brief description of the model and in the next section we present our results and conclusion.

II. MODEL DESCRIPTION

The $su_q(2)$ algebra is a q deformation of the SU(2) Lie algebra and is generated by the operators J_-, J_0, and J_+, which obey the commutation relations [9,10]

$$[J_0, J_\pm] = \pm J_\pm, \quad [J_+, J_-] = [2J_0], \tag{1}$$

with $J_0^\dagger = J_0$, $J_+^\dagger = J_-$, and $[x]$ is the q number defined as

$$[x] = \frac{q^x - q^{-x}}{q - q^{-1}}. \tag{2}$$

[*]alharbi@kacst.edu.sa
[†]alhandi@ksu.edu.sa/hhalhendi@hotmail.com

TABLE I. The fitting parameters and rms of the present models (for $1.0 < c < 1.5$).

	$\mathrm{su}_q(2)$			Modified $\mathrm{su}_q(2)$			
	$\frac{\hbar^2}{2j^{(0)}}$	τ	$\sigma\%$	$\frac{\hbar^2}{2j^{(0)}}$	τ	c	$\sigma\%$
^{191}Au SD1	5.24206	0.00945	0.42239	5.23042	0.00938	1.06323	0.41994
^{191}Au SD2	5.38074	0.01073	0.08715	5.32596	0.01041	1.38868	0.07117
^{190}Hg SD1	5.93895	0.01313	0.58702	5.84574	0.01275	1.45	0.41552
^{193}Hg SD1	5.39158	0.01379	0.17721	5.39158	0.01276	1.02044	0.17721
^{193}Hg SD2	5.29818	0.01004	0.52098	5.22778	0.00965	1.45	0.35778
^{193}Hg SD4	5.29818	0.01004	0.52098	5.22778	0.00965	1.45	0.35778
^{193}Hg SD5	4.83994	0.00219	0.20816	4.81326	0.001	1.17459	0.19576
^{194}Hg SD2	5.28511	0.01007	0.45569	5.20579	0.00958	1.45	0.29270
^{195}Hg SD1	5.26228	0.01035	0.76589	5.19947	0.01004	1.45	0.62843
^{189}Tl SD1	5.52796	0.01065	0.04996	5.49779	0.01042	1.16635	0.03881
^{189}Tl SD2	5.50741	0.01098	0.16131	5.45634	0.01055	1.26928	0.15042
^{191}Tl SD1	5.38536	0.01039	0.05602	5.38353	0.01037	1.01021	0.05593
^{192}Tl SD3	5.1029	0.00890	0.25246	5.03279	0.00827	1.40185	0.18759
^{192}Tl SD4	5.1066	0.00903	0.17178	5.06215	0.00861	1.23881	0.12532
^{193}Tl SD1	5.18845	0.00970	0.27259	5.14984	0.00940	1.21010	0.24470
^{193}Tl SD2	5.18638	0.00889	0.26542	5.12698	0.00839	1.33399	0.21371
^{194}Tl SD1	5.00301	0.00835	0.12796	4.97268	0.00806	1.18518	0.11626
^{194}Tl SD2	5.00398	0.00849	0.08714	4.97817	0.00821	1.13658	0.05851
^{195}Tl SD1	5.2395	0.00950	0.14559	5.23000	0.00942	1.04212	0.13952
^{195}Tl SD2	5.24353	0.01042	0.21265	5.21783	0.01023	1.12423	0.18672
^{193}Pb SD3	5.2603	0.00895	0.19961	5.17564	0.00811	1.45755	0.11696
^{193}Pb SD6	5.34273	0.01056	0.41145	5.25659	0.00985	1.45	0.24225
^{194}Pb SD1	5.62768	0.01231	0.72335	5.50272	0.01128	1.44987	0.40757
^{194}Pb SD2	5.28708	0.01133	0.16664	5.23070	0.01067	1.25752	0.14921
^{194}Pb SD3	5.28808	0.01121	0.13644	5.23187	0.01061	1.27327	0.11896
^{195}Pb SD1	5.05467	0.00596	0.16410	5.00077	0.00496	1.25433	0.06094
^{195}Pb SD4	5.40187	0.01143	0.25481	5.37387	0.01116	1.12594	0.24772
^{196}Pb SD1	5.7067	0.01174	0.23161	5.64178	0.01124	1.26440	0.04316
^{196}Pb SD2	5.42321	0.01111	0.29565	5.34749	0.01039	1.34114	0.23212
^{197}Pb SD1	5.09885	0.00609	0.11375	5.08275	0.00586	1.07249	0.08923
^{198}Pb SD1	5.66046	0.00919	0.33644	5.58475	0.00871	1.45	0.20562

TABLE II. The fitting parameters and rms of the present models (for $1.5 < c < 2.0$).

	$\mathrm{su}_q(2)$			Modified $\mathrm{su}_q(2)$			
	$\frac{\hbar^2}{2j^{(0)}}$	τ	$\sigma\%$	$\frac{\hbar^2}{2j^{(0)}}$	τ	c	$\sigma\%$
^{198}Po SD	5.87348	0.015368	0.37078	5.71292	0.01359	1.52075	0.10810
^{196}Bi SD	5.47304	0.009596	0.61989	5.26217	0.00646	1.82055	0.03724
^{191}Hg SD2	5.28001	0.009649	0.23706	5.18865	0.00899	1.54006	0.08739
^{191}Hg SD3	5.27424	0.010148	0.31120	5.15491	0.00937	1.75194	0.15758
^{193}Hg SD3	5.308	0.010110	0.54763	5.15232	0.00927	1.95203	0.25438
^{194}Hg SD3	5.26475	0.009839	0.55888	5.11966	0.00897	1.88759	0.25922
^{195}Hg SD4	5.08002	0.008086	0.21760	4.98767	0.00753	1.73243	0.13646
^{192}Pb SD	5.73047	0.013809	0.56276	5.5929	0.01268	1.57881	0.47779
^{193}Pb SD4	5.30025	0.010653	0.22269	5.18738	0.00978	1.65015	0.09640
^{193}Pb SD5	5.34677	0.010707	0.36132	5.22763	0.00965	1.58574	0.20445
^{196}Pb SD3	5.4111	0.011044	0.29265	5.29645	0.01002	1.55773	0.15156
^{198}Pb SD3	5.68231	0.011113	0.32830	5.54283	0.00982	1.60574	0.07149
^{194}Tl SD3	5.22953	0.009804	0.30147	5.09825	0.00864	1.72394	0.08790
^{194}Tl SD4	5.23294	0.009887	0.37686	5.08547	0.00847	1.76634	0.12778
^{194}Tl SD5	4.93312	0.008534	0.31105	4.81538	0.00685	1.58204	0.06564
^{194}Tl SD6	4.93169	0.008057	0.24610	4.83214	0.00656	1.50663	0.12430

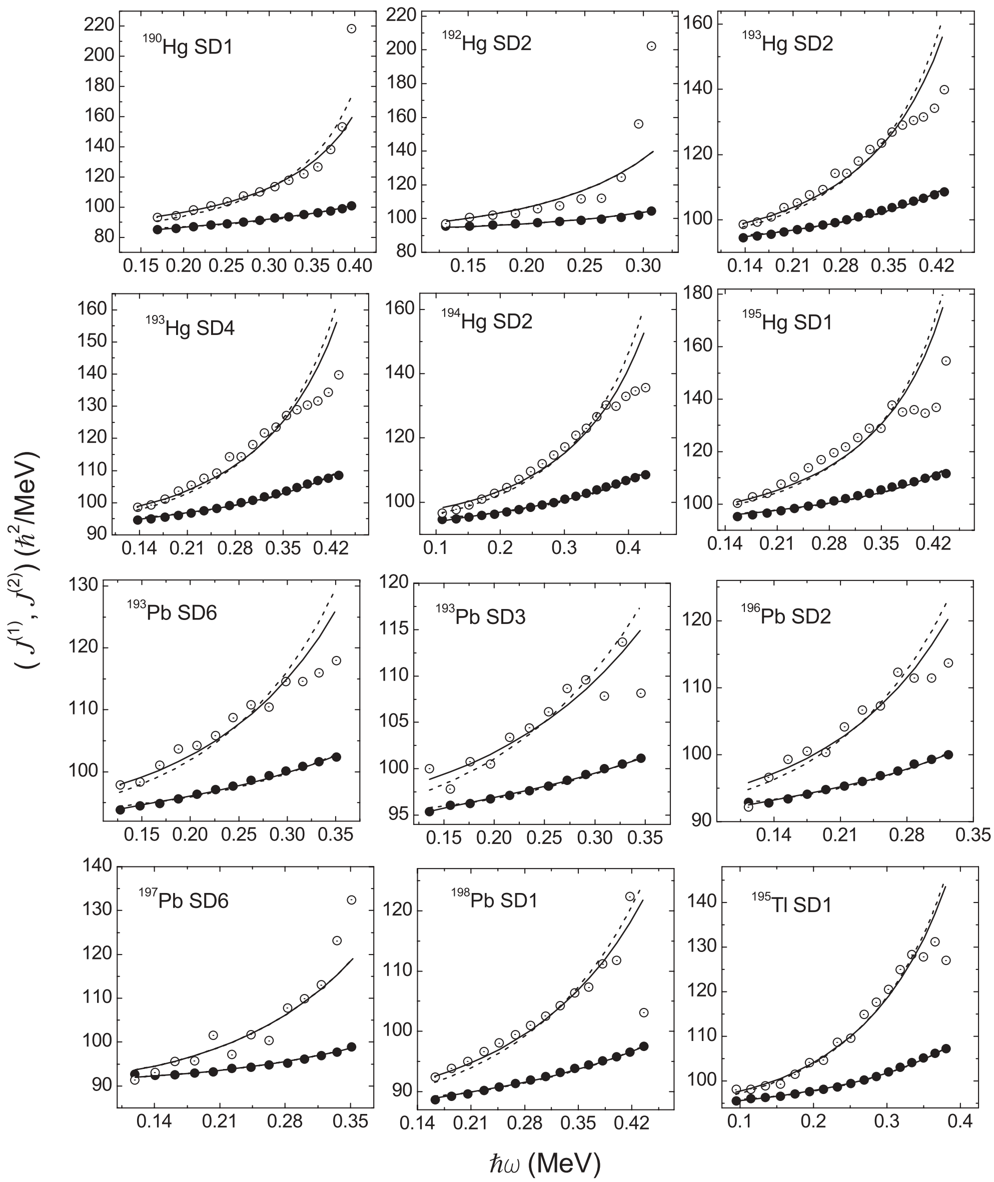

FIG. 1. Comparison between the experimental and theoretical calculations of the kinematic $J^{(1)}$ (dot) and dynamic $J^{(2)}$ (circle) moments of inertia versus the rotational frequency ($\hbar\omega$) of a representative sample of superdeformed bands in the $A \sim 190$ region. The modified su$_q$(2) model (solid line) and the nonmodified su$_q$(2) model (dashed line). ^{192}Hg SD2 and ^{197}Pb SD6 have $c = 1$, and c values for the rest of the SD bands are as shown in Table I.

In terms of the parametrization $\tau = \ln q$, this equation takes the form

$$[x] = \frac{e^{\tau x} - e^{-\tau x}}{e^{\tau} - e^{-\tau}} = \frac{\sinh \tau x}{\sinh \tau}. \tag{3}$$

In the su$_q$(2) formalism it is suggested that rotational spectra of nuclei can be well described by a Hamiltonian proportional to the second-order Casimir operator of the quantum algebra of su$_q$(2) in a manner similar to that of the SU(2) rotator algebra.

The second-order Casimir operator of su$_q$(2) is

$$C_2^q = J_- J_+ + [J_0][J_0 + 1], \tag{4}$$

with eigenvalues $[I][I + 1]$.

A deformed q-like rotor is a quantum system described by the su$_q$(2) invariant Hamiltonian

$$H = \frac{\hbar^2}{2j^{(0)}} C_2^q + E_0, \tag{5}$$

where $j^{(0)}$ is the moment of inertia for $q = 1$ and E_0 is the bandhead energy. The parameters $j^{(0)}$ and E_0 are regarded as constants of the model. The rotational energy spectrum can then be expressed as

$$E = \frac{\hbar^2}{2j^{(0)}} \frac{\sin(I|\tau|)\sin[(I+1)|\tau|]}{\sin^2|\tau|} + E_0, \tag{6}$$

where a pure imaginary $\tau (\equiv \ln q = i|\tau|)$ is assumed.

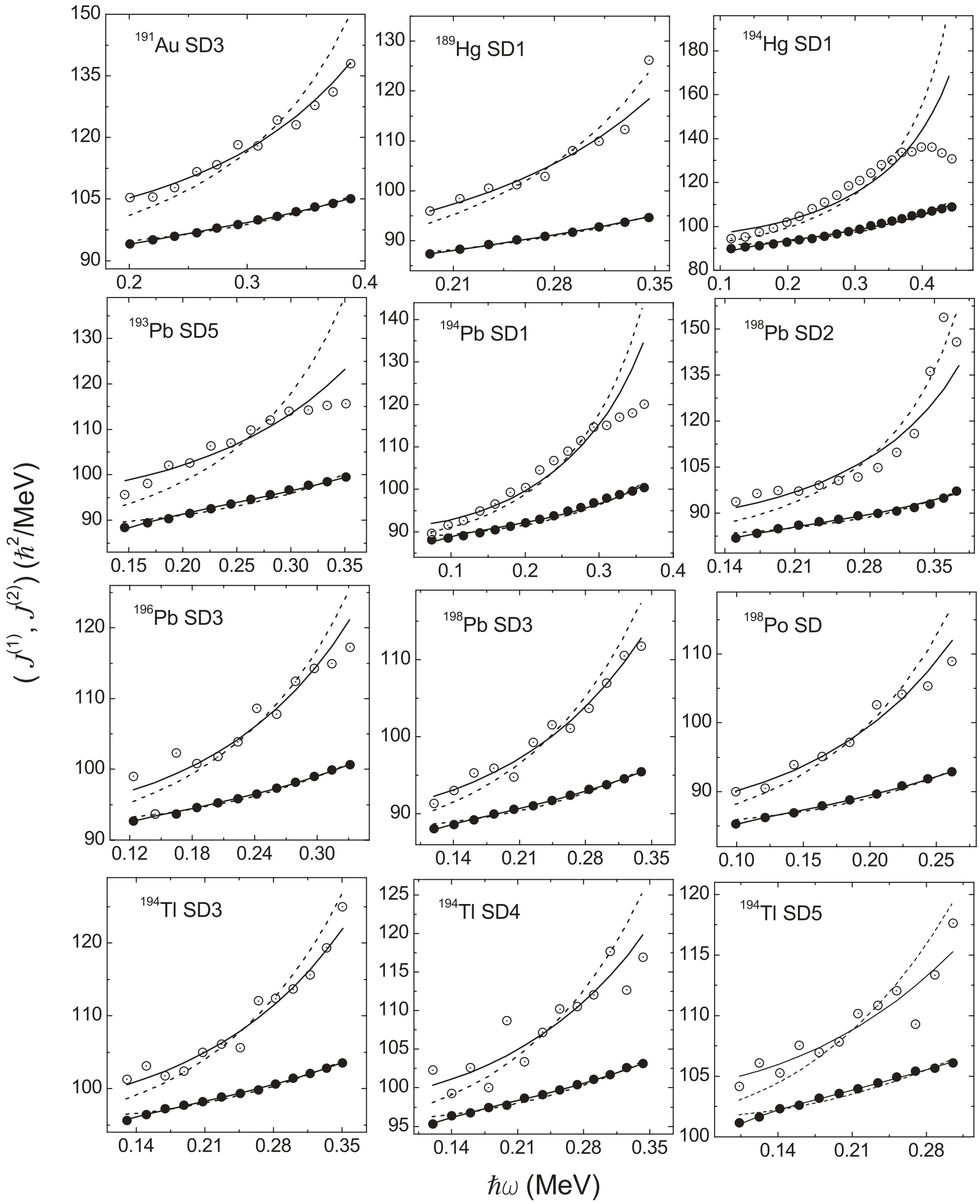

FIG. 2. Comparison between the experimental and theoretical calculations of the kinematic $J^{(1)}$ (dote) and dynamic $J^{(2)}$ (circle) moments of inertia versus the rotational frequency ($\hbar\omega$) of a representative sample of superdeformed bands in the $A \sim 190$ region. The modified su$_q$(2) model (solid line) and the nonmodified su$_q$(2) model (dashed line). ^{191}Au SD3, ^{189}Hg SD1, ^{194}Hg SD1, and ^{198}Pb SD2 have $c =$ 3.35953, 2.39011, 2.47371, and 2.81838, respectively. ^{194}Pb SD1 has c as shown in Table I; and c values for the rest of the SD bands are as shown in Table II.

An extended version of this model is obtained by replacing $I+1$ by $I+c$, where $c>1$. The addition of the parameter c allows for the description of nuclear anharmonicities in a way similar to that of the Interacting Boson Model and the Generalized Variable Moment of Inertia Model. The energy spectrum in this case becomes

$$E = \frac{\hbar^2}{2j^{(0)}} \frac{\sin(I|\tau|)\sin[(I+c)|\tau|]}{\sin^2|\tau|} + E_0, \tag{7}$$

which contains three parameters: the moment of inertia $j^{(0)}$, the deformed parameter τ, and the anaharmonicity parameter c.

In our application of the model, to fit the three parameters in Eq. (7) we make use of the transition energies of 79 SD bands in the $A \sim 190$ region that are reported for the nuclei Au, Tl, Bi, Pb, and Po [5]. The kinematic $J^{(1)}$ and the dynamical moment of inertia $J^{(2)}$ are calculated from the following defining relations

$$J^{(1)} = [(2I-1)/E_\gamma(I)](\hbar^2\,\text{MeV}^{-1}) \tag{8}$$

$$J^{(2)} = 4/[E_\gamma(I+2) - E_\gamma(I)](\hbar^2\,\text{MeV}^{-1}), \tag{9}$$

where the transition energy $E_\gamma(I)$ is

$$E_\gamma(I) = E(I) - E(I-2). \tag{10}$$

We have used as a quantitative measure for best fit the root mean square (rms) σ defined as

$$\sigma = \sqrt{\frac{1}{N}\sum_{I=1}^{N}\left(1 - \frac{E_\gamma^{\text{calc}}(I)}{E_\gamma^{\exp t}(I)}\right)^2}, \qquad (11)$$

where N is the number of levels fitted.

III. RESULTS AND CONCLUSION

A representative sample of the fitting parameters and the rms of the two models, for the studied nuclei, are presented in Tables I and II. Of the 79 superdeformed (SD) bands studied, 20 have the anharmonic parameter $c = 1$; we do not include these bands in the tables because they do not lead to comparison between the two models. These bands are ^{197}Bi SD; ^{190}Hg SD3; ^{191}Hg SD1, SD4; ^{192}Hg SD2, SD3; ^{193}Hg SD6; ^{195}Hg SD3; ^{193}Pb SD2; ^{195}Pb SD2; ^{197}Pb SD2, SD3, SD4, SD5, SD6; ^{192}Tl SD1, SD2; ^{191}Tl SD2; and ^{193}Tl SD3, SD4. In addition 12 SD bands (^{191}Au SD3, ^{189}Hg SD1, ^{190}Hg SD4, ^{192}Hg SD1, ^{194}Hg SD1, ^{195}Hg SD2, ^{190}Tl SD2, ^{193}Tl SD5, ^{193}Pb SD1, ^{195}Pb SD3, ^{196}Pb SD4, and ^{198}Pb SD2) have $c > 2$ and are outside the rotational region [13]. Figures 1 and 2 clearly illustrate that our calculations of the moments of inertia are in good agreement with experimental data at low angular frequency. Both models give good fits for the kinematic moments of inertia but they show marked disagreement for the dynamic moments of inertia at high angular frequency. The models fail to account for the uprising and the downturn of the dynamic moments of inertia. Comparison of the rms of the studied SD bands, Tables I and II, for the two models shows a significant improvement in favor of the generalized su$_q$(2).

ACKNOWLEDGMENTS

We thank the referee for his valuable remarks.

[1] S. M. Polikanov *et al.*, Sov. Phys. JETP **15**, 1016 (1962).
[2] V. M. Strutinsky, Nucl. Phys. **A95**, 420 (1967).
[3] A. Galindo-Uribarri *et al.*, Phys. Rev. Lett. **71**, 231 (1993).
[4] P. J. Twin *et al.*, Phys. Rev. Lett. **57**, 811 (1986).
[5] B. Singh, R. Zywina, and R. B. Firestone, Nucl. Data Sheets **97**, 241 (2002).
[6] D. Ward and P. Fallon, Adv. Nucl. Phys. **26**, 167 (2001); R. Janssens and T. Khoo, Annu. Rev. Nucl. Part. Sci. **41**, 321 (1991).
[7] C. Baktash, B. Haas, and W. Nazarewicz, Annu. Rev. Nucl. Part. Sci. **45**, 485 (1995).
[8] C. A. Stafford and B. R. Barrett, Phys. Rev. C **60**, 051305(R) (1999); D. M. Cardamone, B. R. Barrett, and C. A. Stafford, arXiv:nucl-th/0702072; T. Lauritsen *et al.*, Phys. Rev. Lett. **88**, 042501 (2002).
[9] L. C. Biedenharn, J. Phys. A **22**, L873 (1989); A. J. Macfarlane, *ibid.* **22**, 4581 (1989).
[10] P. P. Raychev, R. P. Roussev, and Yu. F. Simrnov, J. Phys. G: Nucl. Part. Phys. **16**, L137 (1990); S. Iwao, Prog. Theor. Phys. **83**, 363 (1990).
[11] D. Bonatsos *et al.*, J. Phys. G: Nucl. Part. Phys. **17**, L67 (1991); R. S. Johal and R. K. Gupta, J. Phys. G: Nucl. Part. Phys. **25**, L43 (1999).
[12] J. Meng, C. S. Wu, and J. Y. Zeng, Phys. Rev. C **44**, 2545 (1991).
[13] D. Bonatsos, C. Daskaloyannis, A. Faessler, P. P. Raychev, and R. P. Roussev, Phys. Rev. C **50**, 497 (1994).